Russian Journal of Electrochemistry, Vol. 38, No. 1, 2002, pp. 77–87. Translated from Elektrokhimiya, Vol. 38, No. 1, 2002, pp. 90–102.


# Combined Dynamic Model for the Kinetics of Electron Transfer from Cytochrome to a Bacteriochlorophill Dimer in Reaction Centers of *Rps. Sulfoviridis*

**A. I. Kotel'nikov, J. M. Ortega*, E. S. Medvedev, B. L. Psikha, D. Garcia**, and P. Mathis*****

*Institute of Problems of Chemical Physics, Russian Academy of Sciences, Chernogolovka, Moscow oblast, 142432 Russia*

**Instituto de Bioquimica Vegetal y Fotosintesis, Universidad de Sevilla-CSIC, E-41092 Sevilla, Spain*

***DEVM, CEA/Cadarache, B.P. No 1, 13115 St Paul les Durance Cedex, France*

****DBCM-SBE, Bát, 532, CEA/Saclay, 91191 Gif-sur-Yvette Cedex, France*

Received March 15, 2001

**Abstract**—The electron transfer from the heme of cytochrome *c* to the bacteriochlorophill dimer in reaction centers of photosynthetic purple bacteria *Rps. sulfoviridis* is studied by laser flash photolysis at 40–296 K in conditions where one, two, or three cytochrome hemes are chemically reduced. In the model used for the electron transfer kinetics, the protein relaxation is described with a temperature-independent oscillatory coordinate and a temperature-dependent diffusion coordinate, with the protein dielectric relaxation times widely distributed along the diffusion coordinate. It is found that all the protein complexes can be divided into proteins with fast ($k_{et} = 10^7$ to $10^{-4}$ $s^{-1}$) and slow ($k_{et} \ll 100$ $s^{-1}$) electron transfer. These populations presumably differ by the protonation state of the functional group. The contribution of the oscillatory and diffusion coordinates alters, which severely affects $k_{et}$. Parameters $V_{ab}$, $\Delta G$, $\lambda$, $\tau_0$, and $\beta$ for these reactions are determined.

## INTRODUCTION

Reactions of the electron transfer (ET) are key reactions in the operation of many redox proteins, such as reaction centers (RC) of photosynthetic bacteria, nitrogenase, and cytochrome *c* oxidase. Considerable progress has been made in the last few years in quantitative description of reactions of long-range ET between metal-containing centers in native and chemically or genetically modified proteins. Virtually in all publications, these reactions are realized in the framework of a nonadiabatic approximation of the outer-sphere ET theory. In this approximation [1, 2], in conditions of fast reorganization of matrix ($V_{ab}^2 \ll \{\lambda h\nu/4\pi\}$), the ET rate constant $k_{et}^{NA}$ is represented in the form

$$k_{et}^{NA} = k_0^{NA} \exp\left(-\frac{E_a}{RT}\right), \quad (1)$$

where

$$k_0^{NA} = \frac{2\pi V_{ab}^2(R)}{\hbar\sqrt{4\pi\lambda kT}}, \quad (2)$$

$$E_a = \frac{(\Delta G + \lambda)^2}{4\lambda}. \quad (3)$$

Here, $k_0^{NA}$ is a preexponential factor; $E_a$ is the activation energy for an ET reaction; $V_{ab}$ is an overlap integral; $\Delta G$ is the reaction's free energy; while $\lambda$ and $\nu$ are the energy and frequency of nuclear reorganization, respectively. The constant $k_{et}^{NA}$ exponentially depends on the transfer distance $R$ and is independent of $\nu$.

The application of the nonadiabatic approximation depends on the ratio between quantities $\nu$ and $V_{ab}$, which can broadly vary in proteins. For ET in myoglobin, cytochrome *c*, and azurine to distances of 0.8–26 nm, $V_{ab} = 10^{-1}$ to $10^{-3}$ $cm^{-1}$ [3–5]. If nuclear reorganization occurs at the expense of motion of free water molecules with $\nu = 2 \times 10^{12}$ $s^{-1}$ and $\lambda = 1$ eV, the nonadiabatic limit is fulfilled at $V_{ab} \ll 80$ $cm^{-1}$, i.e. for all ET reactions in these proteins [6]. At room temperature, characteristic relaxation frequencies $\nu$ for heme proteins range from $10^8$ to $10^4$ $s^{-1}$ [7–10]. For $\nu = 2 \times 10^4$ $s^{-1}$, the nonadiabatic limit is realized at $V_{ab} \ll 0.8 \times 10^{-2}$ $cm^{-1}$, which is not fulfilled for certain reactions. This is even more probable for the cases where the protein relaxation is hampered by a high viscosity of the solvent or a low temperature. If the nonadiabatic limit is not fulfilled, in accordance with the simplest version of the theory [11, 12], ET is described by the equation

$$k_{et} = \frac{k_0^{NA}}{1 + \frac{k_0^{NA}}{A}\tau} \exp\left(-\frac{E_a}{RT}\right). \quad (4)$$

1023-1935/02/3801-0077$27.00 © 2002 MAIK "Nauka/Interperiodica"

Here, $\tau = 1/\nu$ is the time of dielectric relaxation along the diffusion coordinate of reaction, and $A = \frac{\varepsilon_s}{\varepsilon_\infty}\left(\frac{\lambda}{16\pi kT}\right)^{1/2}$, where $\varepsilon_s$ and $\varepsilon_\infty$ are values of permittivity in static measurements and at high frequencies. If $\frac{k_0^{NA}}{A}\tau \gg 1$, an adiabatic limit is fulfilled:

$$k_{et}^{AD} = \nu A \exp\left(-\frac{E_a}{RT}\right). \quad (5)$$

As seen from (5), the magnitude of $k_{et}^{AD}$ in the adiabatic approximation is determined by molecular dynamics of the environment, which is defined by parameter $\nu$. Moreover, $k_{et}^{AD}$ is independent of the overlap integral $V_{ab}$ and, correspondingly, of transfer distance $R$.

The differences in the functional dependence of $k_{et}$ on $R$ and $\nu$ between nonadiabatic and adiabatic approximations are very important for analyzing ET reactions in proteins, as both $R$ and $\nu$ depend on the steric and dynamic organization of macromolecules and can broadly vary in different proteins. Allowance for this circumstance can be crucial for a correct quantitative analysis of experimental data.

As we have already mentioned in the foregoing, the authors of most publications analyze experimental results in the framework of a nonadiabatic approximation. Its application is based on the experimentally observed fact that $k_{et}$ is dependent on the transfer distance $R$. At present, the researchers use a variety of models that describe how $k_{et}$ depends on the distance between a donor center and an acceptor center. The models ensure good linear correlations between experimentally estimated values of $\log k_0^{NA}$ and parameters that correspond to the effective distance of ET when analyzing reactions in individual proteins, such as RC, myoglobin, cytochrome *c*, or azurine [3, 4, 13–17]. At the same time, when comparing ET in different proteins, all these models fail to provide satisfactory agreement. Such dependences are analyzed in more detail in reviews [18, 19].

Nor can the nonadiabatic approximation explain the experimentally observed fact that the ET rates in heme proteins, azurine, and RC depend on the temperature or viscosity of the solvent. For example, dramatic acceleration of photoinduced ET between a ruthenium complex and zinc-substituted porphyrin in cytochrome *c*, observed at about 125 K, may be attributed to fast oscillatory degrees of freedom [20]. On the other hand, a considerable increase in the rate of similar reactions in myoglobin and hemoglobin, occurring at 170–180 K [21, 22] and even at 220 K for the cytochrome *c*–cytochrome *c* peroxidase complex [23], may be linked with the emergence of slow diffusive motions at temperatures exceeding the glassy point in the protein and solvent.

In myoglobin, the ET from triplet-excited eosin to the protein heme accelerates in the same temperature interval 170–178 K where molecular dynamics, whose time is commensurate with ET, appears at the protein surface [24]. The molecular dynamics in a millisecond range was analyzed from the recorded kinetics of the shift of the eosin phosphorescence spectrum, which reflected a dipole orientation reorganization of the matrix. Subsequent studies showed that the temperature, at which ET accelerated and the phosphorescence spectrum shifted, increased with the solvent viscosity [25]. Thus, the importance of diffusion molecular dynamics and the necessity to evoke an adiabatic approximation for describing ET reactions in heme-containing proteins at low temperatures become evident.

A similar consideration holds true for ET reactions in RC. The temperature effects on the kinetics of ET between proximal heme *c*-559 of a cytochrome subunit and the radical cation of a bacteriochlorophill dimer $P^+$ in *Rps. viridis* were discovered at ambient to helium temperatures [26–30]. The ET rate in RC is also dependent on the viscosity or composition of the solvent [31–33]. As a rule, these effects were explained by the protein structure undergoing modification with variations in the temperature and polarity of the solvent or in the set of hydrogen bonds. However, in reality, the effects could be due to a change in the molecular dynamics of the protein.

The role played by the molecular dynamics of chromatophores in RC and the ET reactions was qualitatively studied with a broad range of physical methods [31, 34–38]. A quantitative description of the ET reaction kinetics and its connection with real physical parameters of the protein structure until very recently were very limited and were done only within a nonadiabatic approximation and ignored parameters that characterize the protein dynamics. In [39], for example, the dielectric behavior of RC in the ET reactions was considered in the framework of the nonadiabatic approximation with use made of dielectric constant $\varepsilon_\tau$, which is time-dependent and, therefore, dependent on the reorganization energy $\lambda$.

An analysis of nonexponential kinetics of ET between a proximal heme and a primary donor in native and genetically modified complexes cytochrome *c*–RC of *Rps. viridis* at different temperatures and reduction states of the cytochrome suggests that the characteristic times of ET in this protein complex can differ by more than four orders of magnitude [26, 30]. Such large differences in the ET rates cannot be explained solely by different distances between the donor and the acceptor or by the temperature-induced variations in parameters $\Delta G$ and $\lambda$ within the nonadiabatic approximation of the outer-sphere transport theory.

The authors of [27–30] analyzed the ET kinetics in RC of *Rps. viridis* in the framework of a multiexponential expansion or with use of effective empirical parameter $Q$, which corresponded to the amplitude of the fast component of a kinetic curve $10^{-5}$ s after the excitation. The temperature dependence of this parameter was explained in [19] within a two-dimensional model for the ET reactions that had been proposed by Ovchinnikova [40] and developed by Sumi and Marcus [41]. It proved possible to explain, within such an approach, the temperature behavior of parameter $Q$ for three cytochrome reduction states in a temperature range extending from 296 to 40 K. The analysis, based on the assumption that the diffusion coordinate is characterized by a single value of the characteristic relaxation time $\tau$, failed to explain the nonexponential shape of the experimentally observed kinetics.

Our goal in this work is to describe temperature dependences of the kinetics of ET from a reduced proximal heme *c*-559 of a cytochrome to the radical cation of a bacteriochlorophill dimer $P^+$ in RC isolated from *Rps. sulfoviridis*, whose characteristics are very similar to those of RC from *Rps. viridis* [42]. Our analysis takes into account specific features of molecular dynamics of the protein, which are due to a wide distribution of relaxation times. To achieve the goal, it was necessary to design a model that would describe dielectric properties of the protein through parameters that characterize its dynamics. Moreover, the parameters should describe the protein state and the rate of ET in different protein states in a universal manner in a wide temperature range.

## EXPERIMENTAL

The RC preparations from *Rhodopseudomonas sulfoviridis*, whose properties are very close to those of RC from *Rps. viridis* were isolated as described in [42]. The absorption kinetics of the preparations after a pulsed excitation with a ruby laser in the time range $10^{-7}$ to $4.5 \times 10^{-3}$ s was studied in different reduction conditions at different temperatures as described in [28], where RC from *Rps. viridis* were investigated. The oxidation of P and its subsequent reduction was measured by recording the absorption of $P^+$ at a wavelength of 1283 nm. The protein preparations were dissolved in 60 vol % glycerol.

## MEASUREMENT AND ANALYSIS OF THE ELECTRON-TRANSFER KINETICS

Kinetic curves of the $P^+$ absorption variation, which describe the ET reaction in RC from *Rps. sulfoviridis* have strictly nonexponential shapes in a wide temperature interval extending from 295 to 40 K and depend on the cytochrome reduction state (Figs. 1, 2), as was shown earlier in similar experiments with RC from *Rps. viridis* [27–30]. As we see in the figures, in the first cytochrome reduction state (only heme *c*-559 is reduced), the ET kinetics perceptibly decelerate in the temperature range 295 to 233 K. With a further decrease in the temperature, kinetic curves practically retain their shape. In the second state of the cytochrome reduction (hemes *c*-559 and *c*-556 are reduced), the temperature range of changes expands to 170 K. In the third reduction state (hemes *c*-559, *c*-556, and *c*-552 are reduced), the ET kinetics slows down even to 40 K (Fig. 2).

Once the primary donor P is excited, the electron is transferred onto the primary acceptor $Q_A$ [43]. Then $P^+$ can undergo reduction at the expense of a direct ET from the reduced proximal heme c-559$^-$ or due to the reverse ET from $Q_A^-$ in accordance with the scheme

$$559^- \xrightarrow{k_{et}} P^+ \xleftarrow{k_r} Q_A^-.$$

While the direct reaction occurs in the microsecond time range, the reverse reaction of ET from $Q_A^-$ to $P^+$ proceeds much slower, specifically, $k_r = 100$–$400\ s^{-1}$ at 100–295 K [44].

A preliminary analysis of the function $F(t) = [P^+](t)/[P^+](0)$, which describes the $P^+$ evolution with the time elapsed after the excitation, shows that all experimental kinetic curves obtained in the time range $10^{-7}$ to $4.5 \times 10^{-3}$ s at various temperatures may be viewed as the sum of two curves whose behavior differs very much (Fig. 1). The initial portions of the curves at $10^{-7}$ to $4 \times 10^{-5}$ s are fast, temperature-dependent, and nonexponential; whereas at $4 \times 10^{-5}$ to $4.5 \times 10^{-3}$ s, the curves drop very slowly and are described by the same exponential function with a constant in the range 100–400 $s^{-1}$. Characteristic rates in the initial portions ($k_{et} = 10^7$–$10^4\ s^{-1}$) are much higher than the rate of reverse reaction $P^+ \leftarrow Q_A^-$. Therefore, we attribute the fast nonexponential portions of these kinetic curves to the reaction c-559$^- \longrightarrow P^+$, while the slow nonexponential portions can be identified with the recombination process $P^+ \leftarrow Q_A^-$.

### *Analysis of the Fast Electron Transfer Kinetics*

**1. Description of the model.** To describe the nonexponential kinetics of ET in RC, we employed a combination of the Ovchinnikova–Sumi–Marcus and Rips–Jortner models. The last model [45] describes the nonexponential kinetics with transition from nonadiabatic to adiabatic ET on the basis of the Cole–Davidson distribution

$$g(\tau) = \frac{\sin(\pi\beta)}{\pi\tau}\left(\frac{\tau}{\tau_0 - \tau}\right)^{\beta}, \quad 0 < \tau < \tau_0,$$
$$g(\tau) = 0, \quad \tau > \tau_0, \tag{6}$$

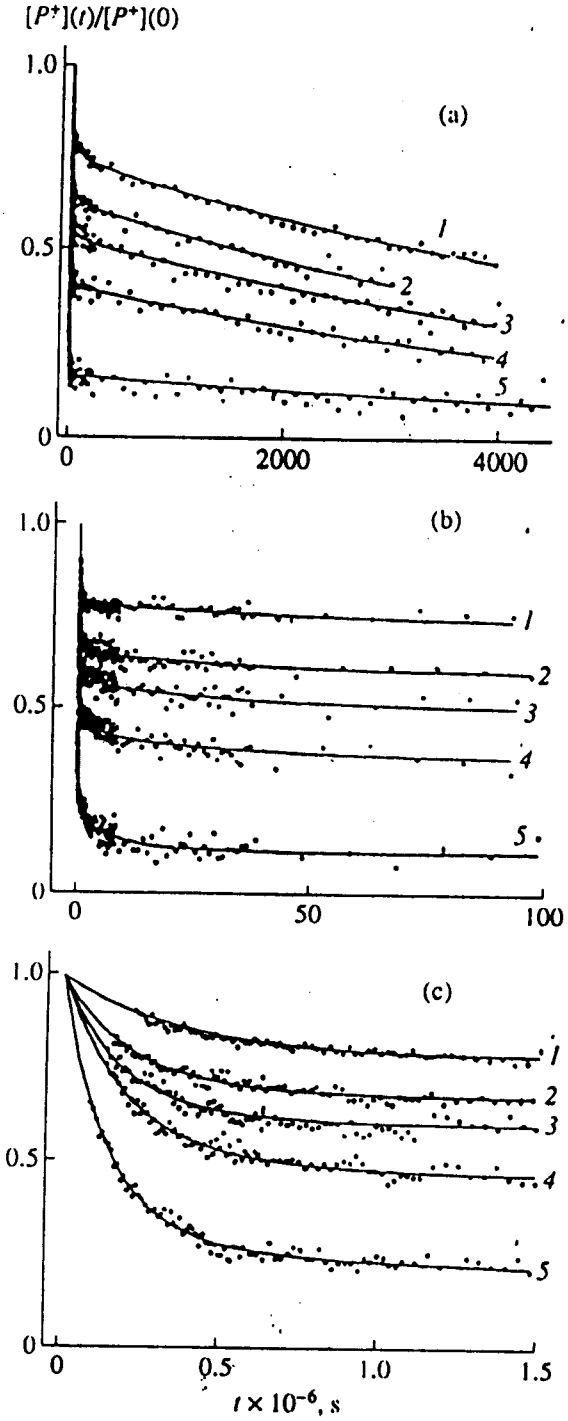


Fig. 1. Kinetics of normalized variations in the absorption of radical cation $P^+$ in RC from *Rps. sulfoviridis* at 1283 nm: (a) in the entire time interval, (b) near $10^{-4}$ s, and (c) near $1.5 \times 10^{-5}$ s, at temperatures of (*1*) 233, (*2*) 248, (*3*) 258, (*4*) 268, and (*5*) 294 K; points represent experimental data and solid lines are computed within the proposed model for cytochrome in the first reduction state at $E_{1/2}$ = 0.360 V (here and in the rest of figures, $E_{1/2}$ is referred to a calomel electrode).

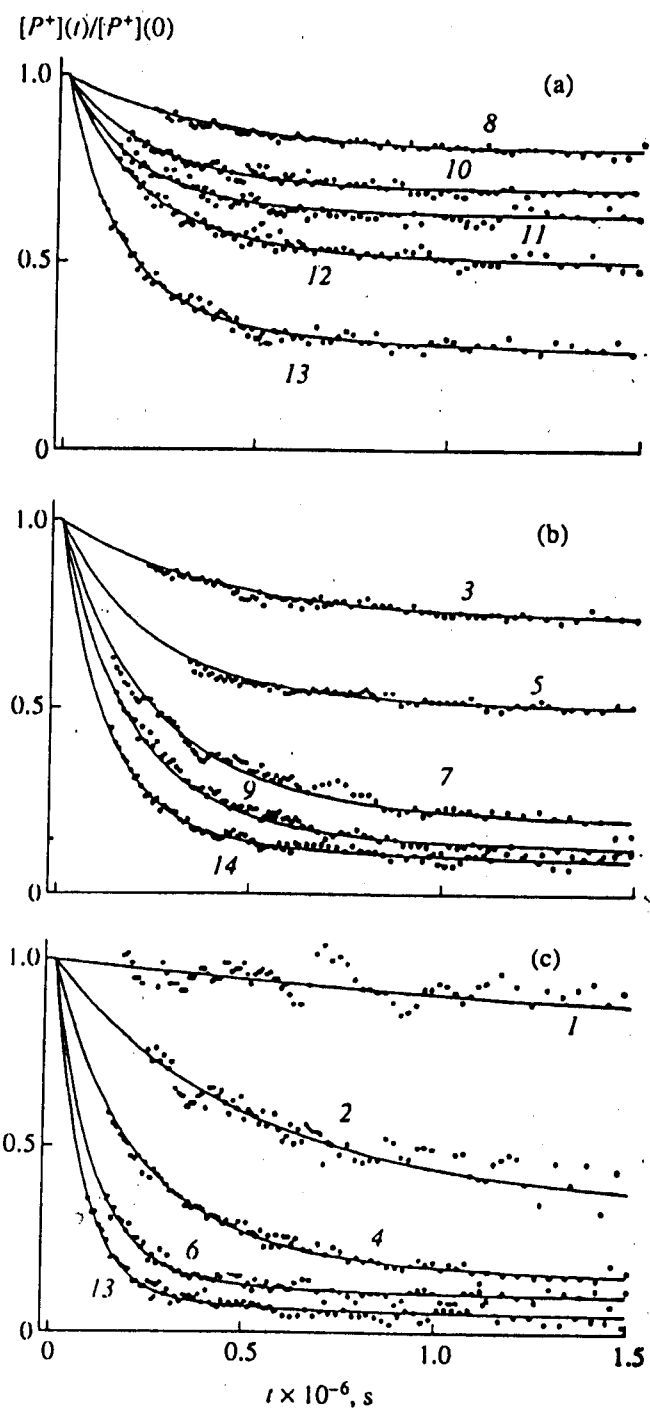


Fig. 2. Kinetics of normalized variations in the absorption of radical cation $P^+$ in RC from *Rps. sulfoviridis* at 1283 nm for the cytochrome in (a) first, (b) second, and (c) third states of reduction in the vicinity of $1.5 \times 10^{-6}$ s at $E_{1/2}$ of 0.360, 0.250, and –0.20 V, respectively, at temperatures of (*1*) 40, (*2*) 147, (*3*) 173, (*4*) 193, (*5*) 195, (*6*) 219, (*7*) 222, (*8*) 233, (*9*) 241, (*10*) 248, (*11*) 258, (*12*) 268, (*13*) 294, and (*14*) 295 K; points represent experimental data and solid lines are computed within the proposed model.

where $0 \le \beta \le 1$ is a Cole–Davidson distribution parameter for a dielectric relaxation spectrum, and $\tau_0$ is the characteristic relaxation time that corresponds to the maximum observed $\tau$. By analogy with the Rips–Jortner approximation, the function $F(t) = [P^+(t)]/[P^+](0)$ may be written in the form

$$F(t) = A_1 \int_0^\infty g(\tau)\exp[-k_{et}(\tau)t]d\tau + A_2\exp(-k_r t), \quad (7)$$

where $k_{et}(\tau)$ is defined by (4). The first integral term in (7) describes the fast direct reaction c-559$^-$ ⟶ P$^+$, the second exponential term is for the reverse reaction P$^+$ ⟵ $Q_A^-$, and coefficients $A_1$ and $A_2$ obey the relation $A_1 + A_2 = 1$.

To be capable of describing the temperature dependences of ET for different cytochrome reduction states in a broad temperature range, we modified (7) as described in [19]. The modifications were based on the Ovchinnikova–Sumi–Marcus model, which assumes that the energy dissipates simultaneously over the oscillatory and diffusion degrees of freedom [40, 41]. Indeed, the diffusion motion in proteins is always accompanied by oscillatory (nondiffusion) motions. Such motions have exceedingly short relaxation times and persist even at very low temperatures. Figure 3 shows a free-energy surface for reactions of this type. If the motion along either coordinate, i.e. the oscillatory coordinate $q$ and diffusion coordinate $x_1$ is fast, the reaction proceeds via optimum, fastest nonadiabatic trajectory *1* from point $B_1$ to point C with a minimum activation energy $E_a^{min}$ at point $S_1$, which represents a transition state of the reaction. However, if the motion along the diffusion coordinate $x_1$ slows down with diminishing temperature and the ET reaction along it becomes formally adiabatic, the effective ET proceeds owing to the possibility for the ET reaction to occur predominantly along the oscillatory coordinate, through another transition state with a higher activation energy. The relaxation process along the oscillatory coordinate is fast and the ET along it is always nonadiabatic (for ET reactions in the microsecond time range). Therefore, the reaction in this case occurs in an adiabatic-nonadiabatic mode along path *2*, which crosses the line of transition states at point $S_2$. Such a shift of transition states can be described phenomenologically by a combination of relations (1) and (4), which describe the ET reaction along the oscillatory and diffusion coordinates, by introducing a $\tau$-dependent preexponential factor and a $\tau$-dependent activation energy

$$k_{et}(\tau) = \sigma(\tau)\exp\left[-\frac{E_a(\tau)}{RT}\right], \quad (8)$$

$$E_a(\tau) = \frac{[\Delta G(\tau) + \lambda]^2}{4\lambda(\tau)}. \quad (9)$$

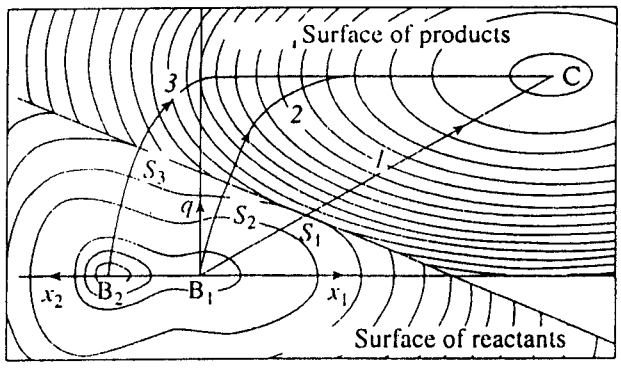


**Fig. 3.** Free energy surface for ET from *c*-559 to P$^+$; axes $q$ and $x_1$ correspond to oscillatory and diffusion reaction coordinates connected with fast component of the ET reaction; axis $x_2$ corresponds to second diffusion coordinate, which provides for transition of protein complex from state $B_1$ to state $B_2$ (see text for explanations).

The $\tau$ dependence may be described by the function

$$\varphi(\tau) = \frac{1}{1 + \frac{k_0^{NA}}{A}\tau}. \quad (10)$$

According to (4), this function serves for switching over between a high-temperature (nonadiabatic) limit and a low-temperature (adiabatic) limit, i.e. between $\varphi(\tau) \sim 1$ at room temperature and $\varphi(\tau) \ll 1$ at low temperatures, respectively. Then, the preexponential factor is

$$\sigma(\tau) = k_0^{NA}[P_\sigma + (1 - P_\sigma)\varphi(\tau)]. \quad (11)$$

where parameter $P_\sigma$ reflects the contribution made by the oscillatory coordinate to the preexponential term. Correspondingly, the quantity $(1 - P_\sigma)\varphi(\tau)$ describes the diffusion coordinate contribution. Similarly, the activation energy in (9) is expressed through the $\tau$-dependent reorganization energy

$$\lambda(\tau) = \lambda[P_\lambda + (1 - P_\lambda)\varphi(\tau)], \quad (12)$$

and the reaction's $\tau$-dependent free energy

$$\Delta G(\tau) = \Delta G[P_G + (1 - P_G)\varphi(\tau)]. \quad (13)$$

In (12) and (13), $P_\lambda$ and $P_G$ are phenomenological parameters, which define temperature-dependent contributions of the oscillatory mode to $\lambda$ and $\Delta G$.

It is necessary to note that the numerator in (9) contains the full reorganization energy $\lambda$, which corresponds to the high-temperature limit in (12) with $\varphi(\tau) = 1$. In the low-temperature limit,

$$E_a(\tau) = \frac{[\Delta G P_G + \lambda]^2}{4\lambda P_\lambda}, \quad (14)$$

where both $P_G$ and $P_\lambda$ are less than unity. As a result, $E_a(\tau)$ decreases with diminishing temperature.

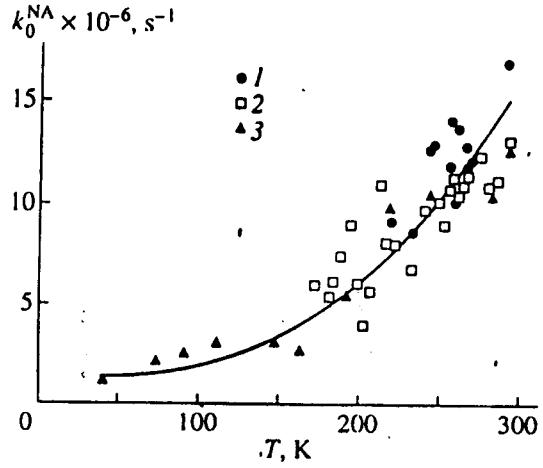


Fig. 4. Temperature dependences of parameter $k_0^{NA}$ for (*1*) first, (*2*) second, and (*3*) third cytochrome reduction states.

We computed kinetic curves for ET with relations (7)–(13) using parameters $P_\lambda = 0.7$ and $P_G = 0.1$, which were determined earlier in [19]. The computer-aided calculations showed these parameters to yield the best results. In the course of a computer-aided fitting, parameter $P_\sigma$ was determined in the range 0.001–0.01. For thermodynamic parameters, we selected quantities from [46], specifically, values of $\Delta G$ for ET in the first, second, and third cytochrome reduction states were –0.14, –0.18, and –0.29 eV, and $\lambda$ was set equal to 0.29 eV for all reactions. As was presumed in [46], the increase in $\Delta G_i$ by 0.04 and 0.15 eV for the second and third reduction states occurred due to electrostatic interaction between the electron on the proximal heme and additional electrons on hemes *c*-556 and *c*-552 undergoing the reduction.

**2. Analysis of the results.** The goal we pursue is to describe the entire ensemble of experimental curves (nearly 50 of these) in the temperature range 40 to 298 K for three cytochrome reduction states in the framework of a unified model. In addition to parameters in equations (1)–(3), which describe nonadiabatic ET, and parameters used in [19] for describing ET within a two-dimensional model, the model we propose here involves a number of new unknown parameters: $\beta$, $\tau_0$, $A_2$, and $k_r$. The model will presumably be a success if parameters $P_\sigma$, $P_G$, and $P_\lambda$, which describe the distribution of the relaxation process between the oscillatory and diffusion modes; parameters $\beta$ and $\tau_0$, which describe the dynamic behavior of the protein; and the preexponential factor $k_0^{NA}$ are the same for all the three cytochrome reduction states. Search for these parameters is made easier by specific features of kinetic curves under study. First, parameters $A_2$ and $k_r$ were determined for each curve from a semilogarithmic dependence in the temperature range $10^{-4}$ to $4.5 \times 10^{-3}$ s. Then, using integral equation (7) at given parameters $P_\sigma$, $P_G$, and $P_\lambda$, each curve was analyzed throughout the entire time interval with the aim of determining parameter $\beta$ and the quantity $\frac{k_0^{NA}}{A}\tau_0$ while minimizing the standard root-mean-square deviation $\Phi$. Quantities $k_0^{NA}$ were determined independently, from initial slopes of experimental curves, taking into consideration the obtained values of $\beta$. Then, using the obtained values of $k_0^{NA}$ and $\frac{k_0^{NA}}{A}\tau_0$, we calculated $\tau_0$. Finally, parameters $\lambda$, $\Delta G$, $P_\sigma$, $P_\lambda$, and $P_G$, taken in pairs, were varied around their initial values, and the value of $\Phi$ was recalculated. As a rule, $\Phi$ assumed a minimum at parameter values taken from [19].

### *The $k_0^{NA}$ Quantity*

This parameter describes the maximum ET rate in a protein in nonadiabatic conditions. In accordance with (2), the magnitude of $k_0^{NA}$ must be the same for all the protein reduction states, provided the cytochrome reduction makes no impact on $V_{ab}$ and $\lambda$.

For all the cytochrome reduction states near ambient temperature, $k_0^{NA} = (1.0–1.6) \times 10^7$ s$^{-1}$ and gradually diminishes to $10^6$ s$^{-1}$ at 40 K (Fig. 4). The reason for the temperature dependence of $k_0^{NA}$ is probably a change in $V_{ab}$ caused by thermal rotational fluctuations, as was shown in [47] for azurine. A change in the fluctuations with temperature alters the efficiency of overlap of wave functions that provide for superexchange between the donor and the acceptor.

The average value of $k_0^{NA} = 1.4 \times 10^7$ s$^{-1}$ can be compared to $k_0 = 10^8$ s$^{-1}$, which was computed from the empirical equation for the model of tunneling through a unidimensional isotropic barrier [15, 16]

$$k_0(s^{-1}) = 10^{16}\exp(-\alpha R). \qquad (15)$$

This equation includes parameter $\alpha = 14$ nm$^{-1}$ and the distance $R = 1.23$ nm between the edges of proximal heme *c*-559 and P$^+$. The agreement between the independently obtained values is good.

Setting $k_0^{NA} = 1.4 \times 10^7$ s$^{-1}$ and using (2), we can calculate $V_{ab}$ for the reaction under study. For $\lambda = 0.29$ eV and $T = 295$ K, $V_{ab} = 0.17$ cm$^{-1}$; this value is commensurate with $V_{ab} = 0.13$ cm$^{-1}$, obtained for a similar reaction between cytochrome $c_2$ and P$^+$ in RC from *Rhodobacter sphaeroides* [48].

### *The β Parameter*

Parameter β characterizes the distribution of dielectric relaxation times of proteins that participate in ET. For all the three cytochrome reduction states, β ~ 0.04–0.06 at 298–220 K (Fig. 5). At low temperatures of 200–130 K, β increases from 0.08 to 0.20 and reaches 0.57 at 40 K.

Direct dielectric measurements give β = 0.55–0.60 for plain glycerol at 198–233 K [49, 50]. Structural fluctuations in 94 vol % glycerol, measured using Mössbauer spectroscopy and analyzed within the Cole–Davidson model, yielded β = 0.65 for 250 K and β ~ 0.3 for 260–275 K [51]. A similar analysis of diffusion shifts of the iron atom in the heme of myoglobin in the crystal structure showed that β dropped from 1.00 to 0.19 with the temperature elevated from 190 to 245 K [52]. It is obvious that β will assume even smaller values at room temperatures, at which measurements by this method cannot be performed. In our experiments, protein complex RC was dissolved in 60 vol % glycerol. And yet, similarly to the Mössbauer measurements in 94 vol % glycerol and in a myoglobin crystal, β drops to a very low level with increasing temperature. The low values of β at room temperatures can be explained by a large contribution of very fast oscillatory or libration motions to the dielectric relaxation of a protein matrix during an ET reaction, with simultaneous existence of a small fraction of proteins that have rather long relaxation times.

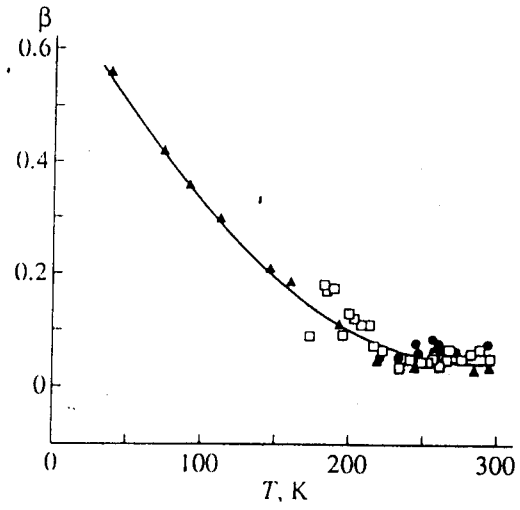


Fig. 5. Temperature dependences of parameter β for three cytochrome reduction states; symbols as in Fig. 4.

### *Adiabatic Factor and Characteristic Times $\tau_0$*

Parameter $\frac{k_0^{NA}}{A}\tau_0$, which was determined directly from our calculations, defines, as follows from (4), the adiabatic nature of the ET reaction for a protein population with a maximum relaxation time $\tau_0$ in the specimen under test. As we have mentioned in the foregoing, the reaction is adiabatic if $\frac{k_0^{NA}}{A}\tau_0$ is much greater than unity. We have found that this parameter equals ten for a protein complex with the cytochrome in the first reduction state at room temperature and increases to 178 with the temperature diminished to 219 K. What this implies is that ET reactions for the protein fraction with maximum relaxation times are essentially adiabatic even at room temperature. At the same time, β = 0.05 for a major fraction of proteins at room temperature, and the average relaxation time $\tau_{av} = \beta\tau_0$ makes the reaction nonadiabatic. Both $\tau_0$ and β increase with decreasing temperature; as a result, the reaction becomes more adiabatic. However, it should be noted that the diffusion coordinate contribution to the ET process fades with a further decrease in temperature, and the ET reaction proceeds predominantly along the oscillatory coordinate in a nonadiabatic mode. If $k_0^{NA}$ is known and the magnitude of parameter $A$ is estimated (setting $\varepsilon_s/\varepsilon_\infty = 2$ and $\lambda = 0.29$ eV), we can determine $\tau_0$; specifically, $\tau_0 = 0.35$ μs at room temperature. As a result, in similar conditions, the average diffusion relaxation time $\beta\tau_0$ in a protein is equal to $17.5 \times 10^{-9}$ s. This sufficiently well coincides with the relaxation time of the heme pocket of myoglobin, which equals $9 \times 10^{-9}$ s, as measured from a recorded relaxation shift of the fluorescence spectrum of the dye incorporated into the heme pocket [53]. A close value of the diffusion relaxation time ($13 \times 10^{-9}$ s) follows also from the extrapolation of two sets of experimental data to room temperatures within the Arrhenius law. The first set includes data on the diffusion mobility of iron atoms in RC with times of $1.4 \times 10^{-7}$ s at 260 K as measured using Mössbauer spectroscopy [46]. The second set consists of data on the dipole relaxation in a triplet-excited eosin environment, the eosin being bound to the myoglobin surface through covalent bonds, in a viscous solvent, with times $10^{-3}$ s at 180 K [24].

### *Average Initial Rate Constants $\tilde{k}_{et}$*

According to the Rips–Jortner approximation [45], if relaxation times in a system obey the Cole–Davidson distribution, a unidimensional diffusion model defines average ET rate constants $\tilde{k}_{et}$ at an initial time instant through the equation

$$\tilde{k}_{et} \sim (1/\tau_0)^{\beta} V_{ab}^{2(1-\beta)} \exp\left(-\frac{E_a}{RT}\right). \qquad (16)$$

In our analysis, we can readily obtain $\tilde{k}_{et}$ from initial slopes of curves under analysis. Values of $\tilde{k}_{et}$ for the three cytochrome reduction states appear in Fig. 6. As

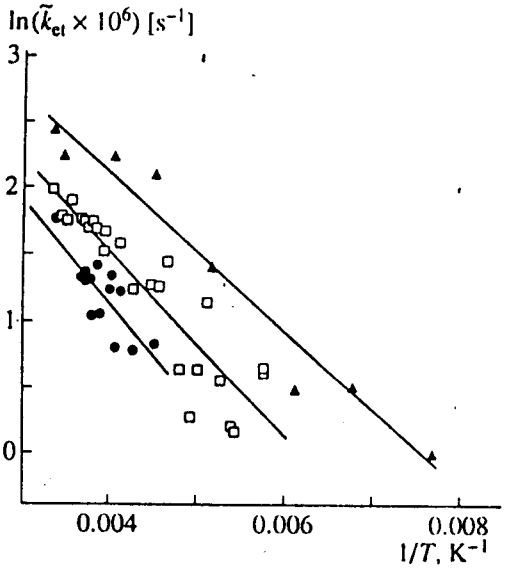


**Fig. 6.** Arrhenius plots for initial average values of rate constant $\tilde{k}_{et}$; symbols as in Fig. 4.

we see, the temperature dependences are linear in the Arrhenius coordinates, with activation energies $\tilde{E}_a^1$ = 0.068 ± 0.015 eV, $\tilde{E}_a^2$ = 0.061 ± 0.006 eV, and $\tilde{E}_a^3$ = 0.051 ± 0.005 eV for the first, second, and third states. These values are a far cry from values $E_a^1$ = 0.019 eV, $E_a^2$ = 0.010 eV, and $E_a^3$ = 0 that follow from (3) at $\Delta G_1$, $\Delta G_2$, and $\Delta G_3$ of 0.14, 0.18, and 0.29 eV, respectively, and $\lambda$ = 0.29 eV. Moreover, these values are much less than the activation energy 0.23 eV for the diffusion shifts inside a protein, which was derived within the Cole–Davidson formalism in [52], which is expected from (5) at $\nu = 1/\tau_0$.

These contradictions are easy to resolve by assuming that the principal contribution to ET at room temperatures is made by the diffusion coordinate. Then, in accordance with (16), the overall activation energy for the average initial constant $\tilde{k}_{et}$ is the sum

$$\tilde{E}_a^i = E_r\beta + E_a^i. \qquad (17)$$

Here, $E_r\beta$ is a fraction of the overall activation energy of the term $(1/\tau_0)^\beta$ in (16), and $E_a^i$ is the Marcusian activation energy with use of $\Delta G_i$ and $\lambda$ in accordance with (3). From (17), using the above values of $\tilde{E}_a^i$ and $E_a^i$, we have $E_r\beta$ = 0.052 eV and obtain $\beta$ = 0.23. The last value is in good agreement with those derived earlier when we analyzed kinetic curves at 130–180 K and with values of $\beta$ obtained in [52] in a Mössbauer spectroscopy study of myoglobin at temperatures of 232–245 K. Values of $\beta$ yielded by an analysis of complete kinetic curves at room temperatures are much smaller. One of the two possible reasons for such a difference is a noticeable contribution of the oscillatory coordinate to the ET process. The other is the contribution of the distribution by relaxation times to the Marcusian activation energy for the ET relation in the framework of our model, which lacks in the Rips–Jortner model.

### *Analysis of the Slow Phase in the Electron Transfer Kinetics*

The proposed model describes all experimental kinetics of ET in a wide temperature range for different reduction states of cytochrome *c*. An in-depth analysis reveals that the first integral term in (7) describes only initial portions of kinetic curves in the time range $10^{-7}$ to $4 \times 10^{-5}$ s. The average instant rate constant, determined from the integral part of (7), equals $10^7$ and $10^4$ $s^{-1}$ for $t$ = 0 and $t = 4 \times 10^{-5}$ s, respectively. For time instants in excess of $4 \times 10^{-5}$ s, the contribution of the integral part of (7) is vanishingly small, and all kinetic curves are nicely described by the exponential term $A_2\exp(-k_r t)$, where $k_r = (1–4) \times 10^2$ $s^{-1}$.

Such a behavior of kinetic curves may be explained by assuming that the specimen contains two protein populations. In the first population, ET from heme *c*-559$^-$ to P$^+$ is fast, with $k_{et} = 10^7$–$10^4$ $s^{-1}$. In this population, the ET kinetics follows our model with the above parameters, and the contribution made by the reverse reaction P$^+$ ⟵ $Q_A^-$ to the P$^+$ reduction is vanishingly small. In the second population, $k_{et}$ of the direct reaction is much less than 100 $s^{-1}$, and the P$^+$ reduction occurs at the expense of the reverse reaction. Coefficients $A_1$ and $A_2$ reflect the fractions of "fast" and "slow" protein populations, and the value of $A_1$ is very close to parameter $Q$ used in [25, 28].

A similar conclusion about the existence of equilibrium between two states of the cytochrome–RC complex (active and inactive toward direct ET onto P$^+$) was drawn in [26] and discussed in [28, 30]. However, two questions remained unresolved. First, why the ET kinetics for the fast and slow protein populations differ that much? Second, why parameters $A_1$ and $A_2$, which describe equilibrium between two populations of the cytochrome–RC complex, vary with the temperature and the cytochrome reduction state (Fig. 7)? For the first state, the fast population converts into the slow one with an activation energy of 0.22 eV (Fig. 7), whereas the activation energy for the third state is a mere 0.031 eV. What is the reason for such a change in equilibrium between the two types of the protein complex during the cytochrome reduction?

The key to solving this mystery is the assumption that there can exist two different protein states, $B_1$ and $B_2$, with a very small difference between free energies (Fig. 3). As coefficients $A_1$ and $A_2$ vary with the temperature and cytochrome reduction state, the difference

between free energies of these two states is likely to be commensurate with the energy of thermal movement and the energy of electrostatic interaction between charges on the proximal heme of cytochrome and added electrons on the neighboring hemes. Estimated on the basis of values used in this work, this difference in energies equals 0.04–0.15 eV, which is close to the energy difference determined from the Arrhenius plots in Fig. 7.

The difference between free energies of protein states $B_1$ and $B_2$ depends on the state of reduction of the cytochrome hemes positioned far away from heme *c*-559. This implies that proteins in these states have different electrostatic charges near the proximal heme. A real physical factor that could give rise to a difference between two such states is the protonation of a carboxyl group near the proximal heme with an activation energy of 0.1 to 0.2 eV.

For example, a carboxyl group in the vicinity of the proximal heme may have a negative charge at room temperature and undergo protonation upon a decrease in the temperature. In the first cytochrome reduction state, a negatively charged carboxyl group creates energetic conditions favorable for fast ET from state $B_1$ to final state C along either path *1* (room temperatures, $k_{et} \sim 10^7\ s^{-1}$) or path *2* (220 K, $10^4\ s^{-1}$). At low temperatures, the carboxyl group undergoes protonation due to the diffusion motion of the proton in the interior of a protein globule with characteristic times $\tau \gg 100$ s, which transfers the protein into state $B_2$ with a decreased electron energy. The system can pass from state $B_2$ into final state C either via the route $B_2 \longrightarrow B_1 \longrightarrow C$ or directly from $B_2$ to C along path *3* with a much higher activation energy (Fig. 3). The ET reaction rate from $B_2$ to C via either path is less than $100\ s^{-1}$.

During the reduction of heme *c*-556, owing to electrostatic interaction between the heme and the proton of a carboxyl group, the equilibrium shifts towards a deprotonated state of the group. As a result, the ET rate increases at a given temperature, and the ET kinetics is observed at lower temperatures. Adding a third electron to heme *c*-552 makes $H^+$ shift farther away from the carboxyl group. This enhances the deprotonation process even further, and ET remains fast at low temperatures. With states $B_1$ (nonprotonated) and $B_2$ (protonated) at equilibrium, the experimentally found difference between free energies is 0.22 and 0.031 eV for, respectively, first and third reduction states (Fig. 7). A free energy change of 0.18 eV is in good agreement with the quantity $\Delta G_1 - \Delta G_3 = 0.15$ eV, which corresponds to the electrostatic contribution into the ET rate increment in fast protein complexes. This fact, discovered by the authors of [46], has been used in our model.

According to a common nonadiabatic approximation or an adiabatic one, a decrease in $\Delta G$ by 0.1 to 0.2 eV (along path 2) at the expense of the electrostatic interaction cannot alter $k_{et}$ by six and more orders of magnitude. Within the Ovchinnikova–Sumi–Marcus

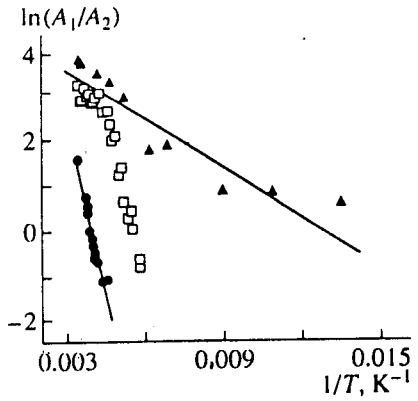


**Fig. 7.** Arrhenius plots for the ratio between parameters $A_1$ and $A_2$, which describe equilibrium between states $B_1$ and $B_2$ of protein complex; symbols as in Fig. 4.

model, variations in the ET rate that large are attributed to a change in the relative contributions of the oscillatory and diffusion degrees of freedom to parameters $\lambda$ and $\Delta G$ according to (12) and (13). Altering a charge state in the course of the carboxyl group protonation may bring about a change in a long-range electrostatic interaction, which defines a contribution to the orientation dipole relaxation. Combining different contributions made by the temperature-independent oscillatory mode and the temperature-dependent diffusion mode to the protein reorganization makes it possible to explain the large difference between ET rates in two protein states at low temperatures.

For an ET reaction in the first cytochrome reduction state, setting $\Delta G_1 = -0.14$ eV, $\lambda = 0.29$ eV, $P_G = 0.1$, and $P_\lambda = 0.7$ and using (10)–(14), we obtain $E_a = 0.02$ eV at room temperature, when $\varphi(\tau) = 1$, and $E_a = 0.1$ eV at a low temperature, when $\varphi(\tau) = 0$. According to (1), this makes the rate constant decrease, upon going from room temperature to 150 K, by approximately three orders of magnitude. With $P_\lambda$ in the other population decreased to 0.2, the activation energy $E_a$ remains the same at room temperature but turns equal to 0.24 eV at a low temperature, which gives a seven-orders-of-magnitude change in the rate constant after lowering the temperature from 295 to 150 K. As a result, for two protein populations with $P_\lambda$ of 0.7 and 0.3, we obtain equal ET rates at room temperatures and preexponential factors that differ by four orders of magnitude at 150 K. For ET at intermediate temperatures, where proteins have a very wide distribution of relaxation frequencies (from fast to exceedingly slow), kinetic dependences are strongly nonexponential.

## CONCLUSION

The new approximation we have employed for ET reactions in proteins takes into account the effect of molecular dynamics on the dielectric relaxation of the protein matrix following a change in the charge state.

To describe the kinetics of ET from c-559$^-$ to P$^+$ in a cytochrome–RC complex in a wide temperature range at different cytochrome reduction states, we employ a phenomenological model. The model allows for the possibility that the protein can undergo relaxation along an oscillatory coordinate and a diffusion coordinate in accordance with the Ovchinnikova–Sumi–Marcus. The model also assumes that characteristic relaxation times are distributed along the diffusion coordinate. Parameters of the model have clear physical meaning and are determined in the course of a computer-aided modeling. The model allows us to put forth a new ET mechanism, which is connected with variations in parameters $\tau_0$, $\beta$, $\lambda$, and $\Delta G$ in conditions where the protein mobility is restricted. Such condition occur in large protein complexes, where the metal-containing active centers are imbedded deep inside the protein globule, following an increase in the solvent viscosity, or a decrease in the temperature. Variation in the diffusion constituent of reorganization energy $\lambda$ is one of the most important, as the energy may alter discretely during local protonation or reduction of groups surrounded by donor and acceptor centers. This opens fresh possibilities for describing large variations if the ET rates in conditions of low dynamics of proteins.

The proposed model manages to describe the ET kinetics in a cytochrome–RC complex under the assumption that there exist two populations of the protein complex. The populations differ by the protonation state of the functional group near heme *c*-559, which makes the ET rate alter by several orders of magnitude. Presumably, this model may come useful for explaining effective direct ET via a system of pigments inside an RC along the right-hand path in the case where ET along the left-hand path is not feasible.

## ACKNOWLEDGMENTS

This work was partially supported by the Russian Foundation for Basic Research; the International Association for Furthering Cooperation between Scientists of Independent States of the Former Soviet Union (INTAS), grant no. 99-00281; and NATO, grant no. LST.CLG.977 814.

## REFERENCES

1. Levich, V.G. and Dogonadze, R.R., *Dokl. Akad. Nauk SSSR*, 1959, vol. 124, p. 123.
2. Marcus, R.A. and Sutin, N., *Biochim. Biophys. Acta*, 1985, vol. 811, p. 265.
3. Casimiro, D.R., Richards, J.H., Winkler, J.R., and Gray, H.B., *J. Chem. Phys.*, 1993, vol. 97, p. 13 073.
4. Casimiro, D.R., Beratan, D.N., Onuchic, J.N., *et al.*, *Mechanistic Bioinorganic Chemistry*, Thorp, H.H. and Pecorado, V.L., Eds., Washington (DC): American Chemical Society, 1995, *Advances in Chemistry Series*, vol. 246, p. 471.
5. Bjerrum, M.J., Casimiro, D.R., Chang, I., *et al.*, *J. Bioenerg. Biomembr.*, 1995, vol. 27, p. 295.
6. Winkler, J.R. and Gray, H.B., *Chem. Rev.*, 1992, vol. 92, p. 369.
7. Blumenfeld, L.A. and Davidov, R.M., *Biochim. Biophys. Acta*, 1979, p. 549; p. 255.
8. Beece, D., Eisenstein, L., Frauenfelder, H., *et al.*, *Biochemistry*, 1980, vol. 19, p. 5147.
9. Bashkin, J.S., Mc Lendon, G., Mukamel, S., and Marohn, J., *J. Phys. Chem.*, 1990, vol. 94, p. 4757.
10. Pierce, D.W. and Boxer, S.G., *J. Phys. Chem.*, 1992, vol. 96, p. 5560.
11. Zusman, L.D., *Chem. Phys.*, 1980, vol. 49, p. 295.
12. Alexandrov, I.V., *Chem. Phys.*, 1980, vol. 51, p. 449.
13. Beratan, D.N., Onuchic, J.N., Betts, J.N., *et al.*, *J. Am. Chem. Soc.*, 1990, vol. 112, p. 7915.
14. Beratan, D.N., Onuchic, J.N., Winkler, J.R., and Gray, H.B., *Science*, 1992, vol. 258, p. 1740.
15. Kotel'nikov, A.I., *Biofizika*, 1993, vol. 38, p. 228.
16. Moser, Ch.C., Keske, J.M., Warncke, K., *et al.*, *Nature*, 1992, vol. 355, p. 796.
17. Siddarh, P. and Marcus, R.A., *J. Phys. Chem.*, 1993, vol. 97, p. 13078.
18. Kotel'nikov, A.I. and Fogel', V.R., *Biofizika*, 1996, vol. 41, p. 596.
19. Kotelnikov, A.I., Vogel, V.R., Pastuchov, A.V., *et al.*, *Biological Electron Transfer Chains: Genetics, Composition, and Mode of Operation*, Canters, G.W. and Vijgenboom, E., Eds., Dordrecht: Kluwer, 1998, *NATO ASI Ser., Ser. C: Math. Phys. Sci.*, 1998, vol. 512, p. 29.
20. Zang, L.H. and Maki, A.H., *J. Am. Chem. Soc.*, 1990, vol. 112, p. 4346.
21. Cowan, J.A., Upmacis, R.K., Beratan, D.N., *et al.*, *Ann. N. Y. Acad. Sci.*, 1988, vol. 550, p. 68.
22. Kuila, D., Baxter, W.W., Natan, M.J., and Hoffman, B.M., *J. Phys. Chem.*, 1991, vol. 95, p. 1.
23. Nocek, J.M., Liang, N., Wallin, S.A., *et al.*, *J. Am. Chem. Soc.*, 1990, vol. 112, p. 1623.
24. Fogel', V.R., Pastukhov, A.V., Psikha, B.L., and Kotel'nikov, A.I., *Biofizika*, 1997, vol. 42, p. 1008.
25. Kotelnikov, A.I., Pastukhov, A.V., Litvinov, P.Yu., and Voskoboinikov, V.L., Abstracts of papers, *18th IUPAC Symp. on Photochemistry*, Dresden, 2000, p. 381.
26. Gao, J., Shopes, R.J., and Wraight, C.A., *Biochim. Biophys. Acta*, 1990, vol. 1015, p. 96.
27. Ortega, J.M. and Mathis, P., *FEBS Lett.*, 1992, vol. 301, p. 45.
28. Ortega, J.M. and Mathis, P., *Biochemistry*, 1993, vol. 32, p. 1141.
29. Ortega, J.M., Dohse, B., Oesterhelt, D., and Mathis, P., *FEBS Lett.*, 1997, vol. 401, p. 153.
30. Ortega, J.M., Dohse, B., Oesterhelt, D., and Mathis, P., *Biophys. J.*, 1998, vol. 74, p. 1135.
31. Noks, P.P., Bystryak, I.M., Kotel'nikov, A.I., *et al.*, *Izv. Akad. Nauk SSSR, Ser.: Biol.*, 1989, vol. 5, p. 651.
32. Paschenko, V.Z., Vasil'ev, S.S., Gorokhov, V.V., Knox, P.P., and Rubin, A.B., *Photosynthesis: From Light to Biosphere*, Mathis, P., Ed., Dordrecht: Kluwer, 1995, vol. 1, p. 491.

33. Paschenko, V.Z., Gorokhov, V.V., Grishanova, N.P., *et al.*, *Biochim. Biophys. Acta*, 1998, vol. 1364, p. 361.
34. Berg, A.I., Noks, P.P., Kononenko, A.A., *et al.*, *Mol. Biol.* (Moscow), 1979, vol. 13, p. 81.
35. Parak, F., Frolov, E.N., Kononenko, A.A., *et al.*, *FEBS Lett.*, 1980, vol. 117, p. 368.
36. Likhtenshtein, G.I. and Kotel'nikov, A.I., *Mol. Biol.* (Moscow), 1983, vol. 17, p. 505.
37. Likhtenstein, G.I., Kulikov, A.V., Kotelnikov, A.I., and Levchenko, L.A., *J. Biochem. Biophys. Methods*, 1986, vol. 12, p. 1.
38. Kochetkov, V.V., Likhtenshtein, G.I., Kol'tover, V.K., *et al.*, *Izv. Akad. Nauk SSSR, Ser. Biol.*, 1984, vol. 4, p. 572.
39. Krishtalik, L.I., *Biochim. Biophys. Acta*, 1996, vol. 1273, p. 139.
40. Ovchinnikova, M.Ya., *Teor. Eksp. Khim.*, 1981, vol. 17, p. 651.
41. Sumi, H. and Marcus, R.A., *J. Chem. Phys.*, 1986, vol. 84, p. 4894.
42. Verméglio, A., Garcia, D., and Breton, J., *Reaction Centers of Photosynthetic Bacteria*, Michel-Beyerle, M.E., Ed., Berlin: Springer, 1989, *Springer Series in Biophysics*, vol. 6, p. 19.
43. Holten, D., Windsor, M.W., Parson, W.W., and Thornber, J.P., *Biochim. Biophys. Acta*, 1978, vol. 501, p. 112.
44. Shopes, R.J. and Wraight, C.A., *Biochim. Biophys. Acta*, 1987, vol. 893, p. 409.
45. Rips, I. and Jortner, J., *Chem. Phys. Lett.*, 1987, vol. 133, p. 411.
46. Frolov, E.N., Goldanskii, V.I., Birk, A., and Parak, F., *Eur. Biophys. J.*, 1996, vol. 24, p. 433.
47. Daizaden, I., Medvedev, E.S., and Stuchebrukhov, A.A., *Proc. Natl. Acad. Sci. USA*, 1997, vol. 94, p. 3703.
48. Venturoli, G., Drepper, F., Williams, J.C., *et al.*, *Biophys. J.*, 1998, vol. 74, p. 3226.
49. Davidson, D.W. and Cole, R.H., *J. Chem. Phys.*, 1950, vol. 18, p. 1417.
50. Davidson, D.W. and Cole, R.H., *J. Chem. Phys.*, 1951, vol. 19, p. 1484.
51. Nienhaus, G.U., Frauenfelder, H., and Parak, F., *Phys. Rev. B: Condens. Matter*, 1991, vol. 43, p. 3345.
52. Chang, I., Hartmann, H., Krupyanskii, Yu., *et al.*, *Chem. Phys.*, 1996, vol. 212, p. 221.
53. Bashkin, J.S., Mc Lendon, G., Mukatel, S., and Marohn, J., *J. Phys. Chem.*, 1990, vol. 94, p. 4757.